Fermi Surface of Superconducting LaFePO Determined from Quantum Oscillations

A. I. Coldea,[1] J. D. Fletcher,[1] A. Carrington,[1] J. G. Analytis,[2] A. F. Bangura,[1] J.-H. Chu,[2] A. S. Erickson,[2] I. R. Fisher,[2] N. E. Hussey,[1] and R. D. McDonald[3]

[1]*H.H. Wills Physics Laboratory, University of Bristol, Tyndall Avenue, Bristol, United Kingdom*
[2]*Geballe Laboratory for Advanced Materials and Department of Applied Physics, Stanford University, Stanford, California 94305-4045, USA*
[3]*National High Magnetic Field Laboratory, Los Alamos National Laboratory, MS E536, Los Alamos, New Mexico 87545, USA*

(Received 4 September 2008; published 20 November 2008)

We report extensive measurements of quantum oscillations in the normal state of the Fe-based superconductor LaFePO, ($T_c \sim 6$ K) using low temperature torque magnetometry and transport in high static magnetic fields (45 T). We find that the Fermi surface is in broad agreement with the band-structure calculations with the quasiparticle mass enhanced by a factor ~2. The quasi-two-dimensional Fermi surface consists of nearly nested electron and hole pockets, suggesting proximity to a spin or charge density wave instability.

DOI: 10.1103/PhysRevLett.101.216402 PACS numbers: 71.18.+y, 74.25.Jb, 74.70.−b

The recent discovery of superconductivity in ferro-oxypnictides [1,2] has generated huge interest as another possible route towards achieving high-T_c superconductivity. LaFePO was among the first Fe-based superconductors to be discovered and has a transition temperature of up to $T_c \approx 7$ K [1]. This compound is isostructural with LaFeAsO, which is nonsuperconducting and has a spin-density-wave (SDW) ground state [3], but becomes a relatively high-T_c superconductor ($T_c \approx 25$ K) when electron doped [4]. By changing the rare-earth ion, T_c reaches 55 K in $SmFeAsO_{1-x}F_x$ (Ref. [2]). Theoretical models suggest that the pairing mechanism in the Fe-based superconductors may be mediated by magnetic fluctuations due to the proximity to a SDW [5–7]. Knowing the fine details of the Fermi surface topology, its tendency towards instabilities, as well as the strength of the coupling of the quasiparticles to excitations is important for understanding the superconductivity.

Quantum oscillations provide a bulk probe of the electronic structure, giving detailed information about the Fermi surface (FS) topology and mass renormalization. To observe quantum oscillations, samples must be extremely clean and the upper critical field must be low enough for the normal state to be accessed; LaFePO is a material which fulfils both these requirements. The tetragonal layered structure of LaFePO is made of alternating highly conductive FeP layers and poorly conducting LaO layers stacked along the c axis [1]; hence, the Fermi surface is expected to be quasi-two-dimensional [8]. Here we report extensive measurements of quantum oscillations in torque and transport data. We find that the Fermi surface of LaFePO is composed of quasi-two-dimensional nearly nested electron and hole pockets with moderate enhancement of the quasiparticle masses.

Single crystals of LaFePO, with dimensions up to $0.2 \times 0.2 \times 0.04$ mm^3, and residual resistance ratios $\rho(300\ \mathrm{K})/\rho(10\ \mathrm{K})$ up to 85, were grown from a tin flux [9]. Single crystal x-ray diffraction gives lattice parameters $a = 3.941(2)$ Å, $c = 8.507(5)$ Å, and La/P positions $z_{\mathrm{La}} = 0.148\,901(19)$, $z_{\mathrm{P}} = 0.634\,77(10)$ in agreement with previous results [1]. Torque measurements were performed with piezoresistive microcantilevers [10] down to 0.3 K on different single crystals from the same batch ($T_c \approx 6$ K): one in Bristol up to 18 T (sample B) and another crystal at the NHMFL, Tallahassee, up to 45 T (sample A). Interplane electrical transport has been measured on a third sample (sample C).

Figure 1(a) shows raw torque measurements versus magnetic field at low temperatures ($T = 0.3$ K) at various angles θ between the magnetic field direction and the c axis [11]. At low fields we observe behavior typical of a bulk anisotropic type-II superconductor in the vortex state [12]. The signal is reversible, indicating weak pinning of vortices. The upper critical field [Fig. 1(a)] is strongly anisotropic, varying between $\mu_0 H_{c2} = 7.2$ T when the magnetic field is parallel to the ab plane and $\mu_0 H_{c2} = 0.68$ T when $B \parallel c$. For magnetic fields above ~9 T, we observe oscillations periodic in inverse field, which arise from the de Haas–van Alphen (dHvA) effect. The oscillatory signal is clearly visible by subtracting a monotonic background (a fifth-order polynomial) from the torque data [dHvA in Fig. 1(b)] or resistivity data [Shubnikov–de Haas effect (SdH) in Fig. 1(c)].

From the fast Fourier transform (FFT) spectra of the oscillatory data [Figs. 1(d) and 1(e)] we can identify the dHvA frequencies F, which are related to the extremal cross-sectional areas A_k, of the FS orbits via the Onsager relation, $F = (\hbar/2\pi e)A_k$. From the evolution of these frequencies as the magnetic field is rotated from being along the c axis ($\theta = 0°$) towards the a axis ($\theta = 90°$) [11], we can construct a detailed three-dimensional picture of the shape and size of the Fermi surface. Four frequencies have significantly larger amplitudes than the others in both samples A and B as shown in Figs. 1(d) and 2(a). We label

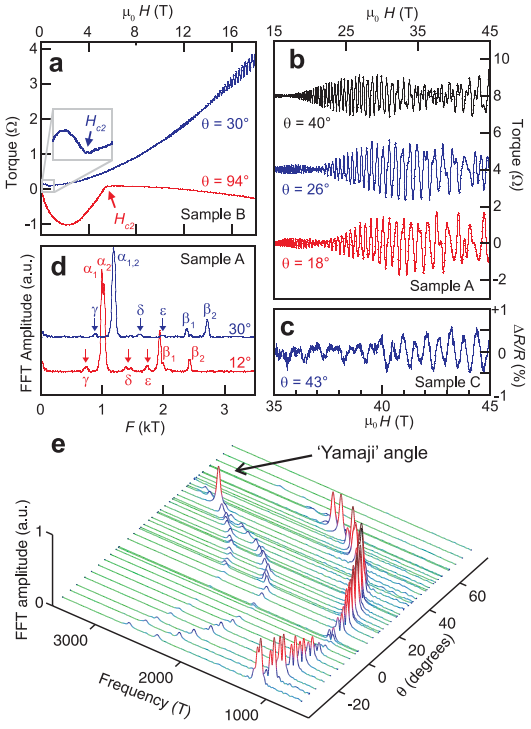

FIG. 1 (color online). (a) Torque measurements on LaFePO measured at $T = 0.35$ K and in magnetic fields up to 18 T for different magnetic field directions. The arrows indicate the position of H_{c2}. (b) Oscillatory part of the torque (dHvA) and (c) resistance (SdH) in magnetic fields up to 45 T. (d) Fourier transform spectra (field range 15–45 T) for two different magnetic field directions. (e) The angle dependence of the Fourier transform spectra for the field range 10–18 T (sample B).

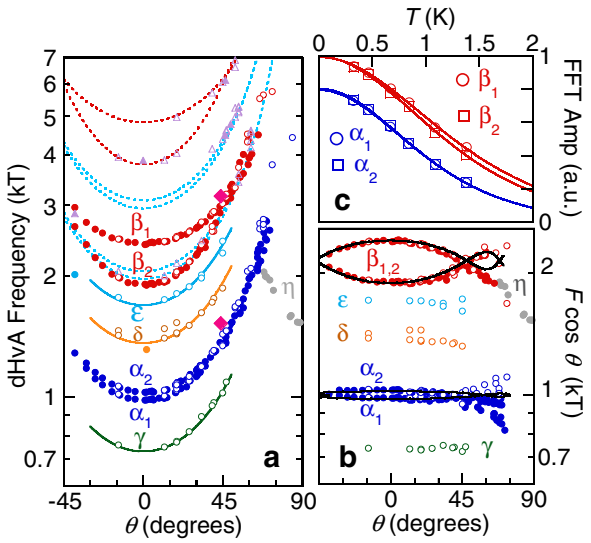

FIG. 2 (color online). (a) Angle dependence of all observed frequencies. Different symbols correspond to sample A (open circles), sample B (filled circles), and sample C (diamonds). Possible harmonics of the main frequencies are shown by triangles and the dashed lines indicate their calculated location. Solid lines are fits to a $1/\cos\theta$ dependence. (b) Angle dependence of $F\cos\theta$. Solid lines are calculations for a simple cosine warped cylinder. (c) The temperature dependence of the Fourier amplitude for $\theta = 32°$ (data are offset for clarity). Solid lines are fits to the Lifshitz-Kosevich formula [15]. The obtained values of the effective mass are listed in Table I.

α_1 and α_2 the two closely split frequencies at $F \approx 1$ kT ($\Delta F \approx 35$ T) and the two higher frequencies, β_1 and β_2. Besides these intense features (and their harmonics [10]), in sample A (which was measured to much higher fields) we see several other frequencies with smaller amplitudes; these are labeled γ, δ, ε and have frequencies in the range 0.7–1.7 kT. An extremely weak signal, η, was observed only in sample B (measured up to 18 T) which we believe originates from a small misaligned crystallite [11]. The observed frequencies correspond to a fraction varying between 2.8% to 9% of the basal plane area of the Brillouin zone. They are significantly larger than those observed in the double-layer Fe-As compound, $SrFe_2As_2$ [13], which is nonsuperconducting, and is likely to have a reconstructed Fermi surface at low temperatures due to a spin-density-wave ground state.

Figures 1(e) and 2(a) show the angular dependence of the main frequencies and their amplitudes. For a purely two-dimensional cylindrical Fermi surface the dHvA frequency varies like $1/\cos\theta$ and deviations from this indicate the degree of c axis warping. As shown in Fig. 2(b), the orbits β_1 and β_2 both originate from sections of FS which have significant warping, but with opposite curvature (i.e., maximal and minimal areas, respectively). The angle dependence of these orbits is well described by Yamaji's analysis of simple cosine warping of a two-dimensional cylinder [14], as is the large increase in the amplitude of the oscillations at $\theta \sim 45°$, where the frequencies cross [see Fig. 1(e)]. These observations indicate that β_1 and β_2 arise from the same FS sheet. For the α orbits the warping of the FS sheet is very small, but the almost identical amplitudes, effective masses (see below), and frequencies strongly suggests that these orbits arise from a single, weakly warped, FS sheet.

The effective mass of the quasiparticles on the various orbits was determined by fitting the temperature dependent amplitude of the oscillations to the conventional Lifshitz-Kosevich formula [15], as shown in Fig. 2(c). The obtained masses range between $1.7m_e$ and $2.1m_e$ and are listed in Table I (m_e is the free electron mass).

We now compare our experimental observations with predictions of the density functional theory calculations of the electronic structure of LaFePO. Our calculations were made using the WIEN2K code with the experimental lattice parameters and atomic positions and including spin-orbit interactions [16]. The resulting band structure is in good agreement with that reported by Lebégue [8]. The density of states at the Fermi level are derived mainly from Fe and P bands suggesting that the carriers flow mainly in the 2D FeP layer. The Fermi surface mainly comprises small, slightly warped tubular sections running along the c direc-

TABLE I. Effective masses (m^*) and frequencies from dHvA data for samples A and B. Calculated band masses (m_b) in LaFePO for shifted and unshifted bands. Orbits are labeled by band number and the location of their center.

	Experiment			Calculations		
		m^*/m_e			m_b/m_e	
Branch	F (kT)	A	B	Orbit	Unshifted	Shifted
α_1	0.985(7)	1.9(2)	1.8(1)	$1Z$	1.0	1.9
α_2	1.025(7)	1.9(2)	1.8(1)	2Γ	0.9	0.7
β_1	1.91(1)	1.7(2)	1.8(1)	$2Z$	1.2	1.1
β_2	2.41(1)	1.8(2)	1.9(1)	3Γ	1.8	1.1
δ	1.36(2)	1.8(3)		$3Z$	2.9	2.5
γ	0.73(2)	1.7(3)		$4M$	0.7	0.7
ϵ	1.69(2)	2.1(3)		$4A$	0.9	0.9
				$5M$	0.8	0.7
				$5A$	0.9	0.8

tion. There are two hole cylinders centered on the Brillouin zone center (Γ) and two electron cylinders centered on the zone corner (M) [see Figs. 3(c)–3(f)]. In addition, there is a small 3D hole pocket centered on Z. The spin-orbit interaction makes small but significant changes to the Fermi surfaces; most notably it breaks the degeneracy of the bands crossing the Fermi level along the XM line such that the two cylindrical Fermi surfaces no longer touch, and it also increases the separation of the elliptical hole pocket and the two cylindrical hole surfaces [Fig. 3(c)].

The frequencies of the extremal dHvA orbits obtained from the calculated band structure are compared with the experimental data in Fig. 3(a). The calculation predicts that there should be 9 frequencies (two for each tube plus one for the 3D hole pocket) in the range 0.7–3 kT (for $\theta \simeq 0°$), which is broadly similar to what is observed experimentally. In particular orbits β_1 and β_2 closely resemble those expected from the larger electron cylinder in both frequency and curvature. The shape and splitting of orbits α_1 and α_2 are similar to that of the smaller electron cylinder. The larger amplitude of these oscillations indicates that they both suffer significantly less damping than the other orbits (we estimate a mean free path of ≈ 1300 and 800 Å for α and β orbits, respectively). This may be a natural consequence of the fact that both of these electron orbits would originate from the same piece of Fermi surface in the larger unfolded Brillouin zone (corresponding to the Fe sublattice [5]). Assuming the above assignment for the α and β frequencies, the three remaining frequencies (γ, δ, ε) would then correspond to hole orbits, although their exact assignment is less clear. For these hole orbits the scattering is a factor ~ 2 larger than the electron orbits [Figs. 1(d) and 1(e)].

Performing small rigid shifts of the energies of the electron and hole bands improves the agreement with experiment. The two bands giving rise to the electron orbits α and β are shifted by -83 and -30 meV, respectively, and the hole bands by $+53$ meV [Fig. 3(b)]. The band that gives rise to the 3D pocket (which we do not observe experimentally) influences significantly the degree of warping along the c axis of the hole cylinders; if this band did not cross the Fermi level we would have a better agreement between our data and calculations [Figs. 3(a) and 3(b)].

A two-dimensional cut in the ΓXM plane for our calculated unshifted and shifted Fermi surface [see Figs. 3(e) and 3(f)] shows that the electron pockets at the corner of the Brillouin zone (M) have almost similar shapes and sizes to the hole pockets at the center of the zone (Γ). Nesting requires a perfect match between the size and the Fermi surface topology of the electron and hole pockets and this could stabilize a spin-density wave (magnetic order) or charge-density wave (structural order) with a wave vector $\mathbf{Q} \approx [\pi, \pi, 0]$ [6,7,17]. LaFePO is nonmagnetic [18] but importantly our results suggest that size and the shape of the electron and hole pockets are indeed very similar [Figs. 3(e) and 3(f)] implying that LaFePO may be

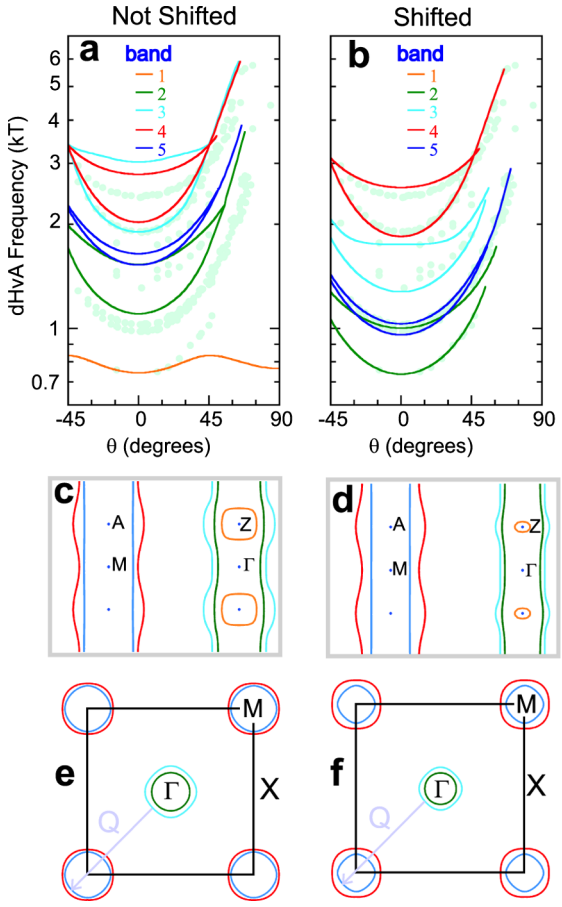

FIG. 3 (color online). (a) Calculated dHvA frequencies versus angle for unshifted bands compared to experimental data (filled circles). (b) As in (a) but for shifted bands (see text). (c),(d) Two-dimensional (110) cuts of the Fermi surface and (e),(f) two-dimensional cuts in the ΓXM plane (001) for unshifted and shifted bands, respectively. Solid black lines indicate the Brillouin zone. A possible interband nesting vector, $\mathbf{Q} \approx [\pi, \pi, 0]$, between electron and hole bands is shown.

close to nesting and hence to a spin or charge density wave instability.

For undoped LaFePO the volume of the electron and hole sheets is equal (compensated metal), but shifting the bands (as described above) creates an imbalance of ~ 0.034 electrons per formula unit. A possible explanation for this imbalance can be related to a small amount of electron doping in our crystals due to an oxygen deficiency of $\sim 1.7\%$ which is below the resolution of our x-ray data.

The band-structure calculation allows us to estimate the many-body (electron-phonon and electron-electron) enhancements of the quasiparticle masses over their band values. Table I shows the band masses for all the predicted orbits as calculated, and after application of band shifts. For the identified bands a moderate renormalization is found, with $m^*/m_b = (1 + \lambda) \approx 2$. For the hole orbits the calculated frequencies do not correspond exactly to the experimental ones, however, as the band masses for most of the hole orbits are in the range 0.7–$1.1 m_e$ and the measured m^* values are $\approx 2m_e$, a similar level of enhancement is likely. Reported measurements of the electronic specific heat coefficient (γ) vary between 7–12 $\mathrm{mJ/mol\,K^2}$ [9,18,19]. In 2D materials γ can be estimated from the renormalized dHvA masses, summed over all of the observed FS sheets. Four quasi-2D FS sheets with an effective mass $\sim 2m_e$ would give $\gamma_{\mathrm{dHvA}} \sim 6\ \mathrm{mJ/mol\,K^2}$, close to the lower end of the experimentally observed values, without including any contribution from a 3D pocket.

A recent angle-resolved photoemission spectroscopy (ARPES) study of LaFePO [20] showed an electronlike FS pocket centered at the M point and two hole sheets at the Γ point. The electron sheet and the smaller hole orbit have areas close to the experimentally observed dHvA frequencies. When compared to band-structure calculations, the bands found in the ARPES measurements are renormalized by a factor two, similar to the mass enhancements we have found. This suggests that the renormalization occurs over the whole band, rather than being localized to energies close to the Fermi level, as found in Sr_2RuO_4, [21]. One of the hole pockets seen in ARPES is much larger (>12 kT) than any dHvA frequencies observed here; its presence creates a significant charge imbalance of one electron per unit cell, suggesting that this feature is related to surface effects [20].

As in the other ferrooxypnictides, in LaFePO the band structure is very sensitive to the position of the P atom [17,22]. Considering the P atom in the position optimized (the ''relaxed'' structure) results in hole orbits which are much too *small* to explain our data. Much larger band energy shifts are needed to bring it into approximate agreement and we find that the band structure calculated with the experimental P position provides a better description of the data.

In conclusion, we have found experimentally that the Fermi surface of the superconductor LaFePO is in broad agreement with band-structure calculations with a mass enhancement of about 2 due to many-body interactions. The difference in amplitudes of the dHvA signal between the hole and electron pockets is an indication of different scattering rates affecting these orbits. The near-perfect matching between the hole and the electron orbits that we observe suggests that LaFePO may be close to a spin- or charge-density wave transition and that magnetic fluctuations are an important ingredient in the physics of the Fe-based superconductors.

We thank E. A. Yelland, N. Fox, and M. F. Haddow for technical help and I. Mazin for helpful comments. This work was supported financially by EPSRC (U.K.) and the Royal Society. A. I. C. is grateful to the Royal Society for financial support. Work at Stanford was supported by the U.S. DOE, Office of Basic Energy Sciences under contract DE-AC02-76SF00515. Work performed at the NHMFL in Tallahassee, Florida, was supported by NSF Cooperative Agreement No. DMR-0654118, by the State of Florida, and by the U.S. DOE.

[1] Y. Kamihara *et al.*, J. Am. Chem. Soc. **128**, 10 012 (2006).
[2] Z.-A. Ren *et al.*, Chin. Phys. Lett. **25**, 2215 (2008).
[3] C. de la Cruz *et al.*, Nature (London) **453**, 899 (2008).
[4] Y. Kamihara *et al.*, J. Am. Chem. Soc. **130**, 3296 (2008).
[5] I. I. Mazin *et al.*, Phys. Rev. Lett. **101**, 057003 (2008)
[6] A. V. Chubukov, D. Efremov, and I. Eremin, Phys. Rev. B **78**, 134512 (2008).
[7] V. Chetkovic and Z. Tesanovic, arXiv:0804.4678.
[8] S. Lebègue, Phys. Rev. B **75**, 035110 (2007).
[9] J. Analytis *et al.*, arXiv:0810.5368.
[10] Changes in lever resistance were measured with a Wheatstone bridge circuit. The sensitivity of the levers is approximately 0.1° per Ohm. At certain angles and at the highest fields, the deflection of the cantilever is large enough to generate harmonics of the main dHvA frequencies.
[11] The x-ray Laue diffraction indicates that the exact axis of rotation between is ~35° (sample *A*) and ~14° (sample *B*) from the *a* axis; a small piece of crystal with its *c* axis oriented 73° away from that of the main piece of the crystal was detected in sample *B*.
[12] Z. Hao and J. R. Clem, Phys. Rev. B **43**, 7622 (1991).
[13] S. E. Sebastian *et al.*, J. Phys. Condens. Matter **20**, 422203 (2008).
[14] K. Yamaji, J. Phys. Soc. Jpn. **58**, 1520 (1989).
[15] D. Shoenberg, *Magnetic Oscillations in Metals* (Cambridge University Press, Cambridge, England, 1984).
[16] P. Blaha *et al.*, WIEN2K, an augmented plane wave + local orbitals program for calculating crystal properties, edited by Karlheinz Schwarz, Technica Universität Wien, Austria, 2001. We used 10^4 k points (in the full Brillouin zone) for convergence and 10^5 k points for the FS calculations and the GGA96 exchange correlation potential.
[17] I. I. Mazin *et al.*, arXiv:0806.1869.
[18] T. M. McQueen *et al.*, Phys. Rev. B **78**, 024521 (2008).
[19] Y. Kohama *et al.*, J. Phys. Soc. Jpn. **77**, 094715 (2008).
[20] D. H. Lu *et al.*, Nature (London) **455**, 81 (2008).
[21] N. J. C. Ingle *et al.*, Phys. Rev. B **72**, 205114 (2005).
[22] V. Vildosola *et al.*, Phys. Rev. B **78**, 064518 (2008).